Lévy Based Cross-Commodity Models and Derivative Valuation*

Sebastian Jaimungal [a] and Vladimir Surkov [b]

[a]Department of Statistics,
University of Toronto, Toronto, Canada
sebastian.jaimungal@utoronto.ca

[b]The Fields Institute for Research in Mathematical Sciences and
Department of Statistics, University of Western Ontario, London, Ontario
vladimir.surkov@utoronto.ca

Energy commodities, such as oil, gas and electricity, lack the liquidity of equity markets, have large costs associated with storage, exhibit high volatilities and can have significant spikes in prices. Furthermore, and possibly most importantly, commodities tend to revert to long run equilibrium prices. Many complex commodity contingent claims exist in the markets, such as swing and interruptible options; however, the current method of valuation relies heavily on Monte Carlo simulations and tree based methods. In this article, we develop a new cross-commodity modeling framework which accounts for jumps and cointegration in prices and introduce a new derivative valuation methodology by working in Fourier space. The method is based on the Fourier space time stepping algorithm of Jackson, Jaimungal, and Surkov (2008), but is tailored for mean-reverting models. We demonstrate the utility of the method by applying it to European, American and barrier options on a single commodity, to European and Bermudan spread options on two commodities and to a particular class of swing options.

*SJ thanks NSERC of Canada for partially funding this work. The authors wish to thank two anonymous referees for very useful comments which helped to improve the article.

Electronic copy available at: http://ssrn.com/abstract=1302887

1. Introduction

Energy commodities, such as oil, gas and electricity, lack the liquidity of equity markets, have large costs associated with storage, and exhibit high volatilities. Perhaps even more importantly, commodities tend to revert to long run equilibrium prices. Moreover, commodities exhibit cointegration in prices, particularly those of a raw commodity and its refined products. Like equity prices, they are also exposed to sudden price jumps; however, unlike equity prices, electricity prices in particular are prone to large price spikes (orders of magnitudes higher than typical jumps) which quickly revert to the mean. These stylized empirical facts are well documented in, for example, Clewlow and Strickland (2000), Eydeland and Wolyniec (2003) and Benth, Benth, and Koekebakker (2008).

Gibson and Schwartz (1990), Cortazar and Schwartz (1994) and Schwartz (1997) were the first to use an Ornstein-Uhlenbeck (OU) process to model commodity prices and value forward contracts on those commodities. Clewlow and Strickland (2000) propose a jump-diffusion extension of the OU process for modeling spot prices, while Cartea and Figueroa (2005) employ a similar model to value electricity forward contracts. Further, Hikspoors and Jaimungal (2007) derive closed form formulae for spread options using single-factor and two-factor OU processes,while Benth, Kallsen, and Meyer-Brandis (2007) study a multi-factor (but single commodity) arithmetic commodity model.

In this article, we first introduce a multifactor cross-commodity model in Section 2 with Lévy drivers, and explore how it captures many standard commodity models. The framework is, however, more general and allows for multiple sources of jumps together with differing mean-reversion scales as well as cointegration of price series. To illustrate the model's flexibility, we explore some new and interesting specifications. Our model is related to, but distinct from, Benth, Kallsen, and Meyer-Brandis (2007) who study a multi-factor (but single commodity) arithmetic model for prices and Paschke and Prokopczuk (2008) who introduce a multi-factor gaussian model. Benth, Kallsen, and Meyer-Brandis (2007) focus on simple European claims, while Benth and Kufakunesu (2009) further analysis this model for Asian and spread option valuation. Paschke and Prokopczuk (2008) focus on calibrating their model to futures price data and do not value derivatives. The authors find evidence that cointegration in price series is an important factor, and demonstrate the obvious fact that if cointegration is included, then the risk associated with long term commodity cash-flows is much lower than if cointegration is absent. Our model includes these models as special cases as well as other more general models.

Based on our model, we develop an FFT methodology for valuing general contingent claims. One of the motivations is to value highly path-dependent claims such as Bermudan spread options, American styled swing options and storage options (see e.g. Eydeland and Wolyniec (2003)). Traditional approaches use either finite difference discretizations or least-squares Monte-Carlo à la

Electronic copy available at: http://ssrn.com/abstract=1302887

Carriere (1996) and Longstaff and Schwartz (2001). For an overview of swing options and current valuation methods see Ware (2005). More recently, Chen and Forsyth (2007) use a regime switching model to value storage options; however, they resort to a coupled finite difference scheme and do not incorporate jumps in prices. Our methodology easily extends to the regime switching case, while maintaining the efficiency of FFT, and trivially incorporates jumps.

In our framework, the commodity spot price is driven by a mean-reverting jump-diffusion process. The discounted and log-transformed option price process then satisfies a partial integro-differential equation (PIDE) which must be solved numerically in most cases. To value barrier options, additional boundary conditions along the barrier(s) supplement the PIDE. To value American or Bermudan styled options, the PIDE is satisfied only in the continuation region and the optimal exercise point must be searched for at each time step. In the absence of jump components, the resulting pricing PDE can be discretized using standard divided differences to approximate the first and second order derivatives. Whether the approximation scheme is carried out explicitly, implicitly or through a weighted scheme, the resulting system is tri-diagonal and leads to very efficient numerical approximations. Unfortunately, when jumps are present, the integral term in the PIDE must be approximated resulting in a dense matrix structure. Several methods for dealing with this issue have been presented in the literature with most relying on the explicit evaluation of approximations to the integral term in conjunction with an iterative refinement and possibly FFT speedup.

Andersen and Andreasen (2000) propose an FFT-Alternating Direction Implicit (FFT-ADI) method which treats the diffusion and integral terms symmetrically over a full time step by splitting the time step into two half-steps; an explicit scheme is used on the first half-step and implicit scheme on the second half-step. The inversion of the dense matrix is performed efficiently by regarding the integral term as a convolution and utilizing the FFT algorithm. The fixed point iteration scheme of d'Halluin, Forsyth, and Vetzal (2005) treats the integral term explicitly while iterating to attain the required error tolerance per time-step. In addition, Implicit-Explicit (IMEX) Runge-Kutta schemes have been applied in Briani, Natalini, and Russo (2004) to solve the PIDEs. Although the FFT algorithm is frequently used to speed up the computation of the integral term, such schemes require careful mapping of function values between the diffusion and integral grids. Furthermore, all of the above prescribed schemes were developed without mean-reversion, although they could in principle be made to work with mean-reversion.

Recently, purely FFT-based algorithms have gained traction due primarily to their efficiency and also since they only require the characteristic function of the log price. Further, for many popular models, the characteristic function is available in simple, closed form, even though the density function is not. The first approach to make full use of the FFT method appears in Carr and Madan (1999) where they obtain European option values for a range of strike prices. The

method requires an analytic expression for the Fourier transform of the option payoff as a function of log-strike and then utilizes the FFT algorithm to obtain prices. Jackson, Jaimungal, and Surkov (2008) develop a Fourier Space Time-stepping (FST) algorithm that is based on the solution of the PIDE in Fourier space while Lord, Fang, Bervoets, and Oosterlee (2008) develop a similar method (called CONV) by utilizing the convolution property of Fourier transforms. The advantage of the FST method (as well as the CONV approach) is that it does not require an analytic expression for the Fourier transform of the option value function, and thus can be readily applied to pricing of options with non-standard payoffs. Moreover, by obtaining option values for a range of spot prices, rather than strike prices, the authors develop a time-stepping scheme enabling pricing of path-dependent options, such as Bermudan, American, and barrier options.

With mean-reversion, the characteristic exponent of the commodity price process is state dependent and the above methods cannot be readily applied to pricing of path-dependent or early-exercise options. In this paper we extend the FST method of Jackson, Jaimungal, and Surkov (2008) to handle mean-reverting processes and demonstrate how the method can efficiently price European, Bermudan, American, barrier and swing options. We coin this the *mean-reverting Fourier Space Time-Stepping* (mrFST) method. The method retains all of the advantages of the original FST method: European options can be priced using a single time-step to obtain option values for a range of spot prices, Bermudan options do not require time-stepping between monitoring dates, and the method can be readily extended to the multi-asset and regime switching framework.

The remainder of this article is organized as follows. In Section 2 we introduce our multi-factor cross-commodity model and demonstrate how it reduces to some well known models as well as providing some new specifications. Here, we also provide the main pricing result for European options and determine forward prices. In Section 3 we develop the mrFST method and explore some of its properties for the examples introduced in Section 2. In Section 4 we carry out several numerical experiments and compare our results with Monte Carlo estimates. In Section 5 we apply the mrFST method to pricing of swing options and some concluding remarks are made in Section 6. The Appendix contains convergence tables, a proof of the main pricing result and defines a class of risk-neutrals which preserves the structure of the real-world model.

2. Mean-Reverting Jump Models for Commodities

We model the logarithms of n commodity spot-prices $\mathbf{X}(t)$, rather than the spot-prices $\mathbf{S}(t)$ directly[2], as a linear transformation of a set of $d-$fundamental market factors $\mathbf{Y}(t)$, which themselves are driven by the continuous time counterpart of a VAR(1) model. In the discrete setting,

[2]In principle, it is also possible to develop an arithmetic spot price model as in Benth, Kallsen, and Meyer-Brandis (2007) by viewing $\mathbf{X}(t)$ as the collection of spot-prices rather than logarithm of spot-prices.

the fundamental market factors evolve according to the time-series model

$$\mathbf{Y}(t+1) - \mathbf{Y}(t) = -\boldsymbol{\kappa}\mathbf{Y}(t) + \boldsymbol{\epsilon}(t) \,, \tag{1a}$$

$$\mathbf{X}(t) = \boldsymbol{\theta}(t) + \mathbf{B}\,\mathbf{Y}(t) \,. \tag{1b}$$

Here, $\boldsymbol{\kappa}$ is a $d \times d$ matrix with positive eigenvalues representing the mixing of the market factors, $\boldsymbol{\theta}(t)$ is an n-dimensional vector representing the long-run means, $\mathbf{B}$ is a $d \times n$ matrix representing the linear transformation of the market factors into the observed log-prices, and $\boldsymbol{\epsilon}(0), \boldsymbol{\epsilon}(1) \ldots$ are i.i.d. d-dimensional noise vectors (possibly heavy tailed) which, in the continuous time model, will be modeled via a Lévy process. Since seasonality effects are known to affect prices of certain commodities, such as electricity and heating oil, we allow $\boldsymbol{\theta}(t)$ to be time dependent. There are many approaches to modeling seasonality; however, we do not specify a particular form for this factor as it plays no key role in the development of the algorithm, and in the examples used throughout we will in fact set it to a constant.

Notice that only when $n = d$ and $\mathbf{B}$ is invertible are the processes $\mathbf{Y}(t)$ available from the observed prices $\mathbf{X}(t)$. As such, if $\mathbf{Y}(t)$ are unobservable, the model is in general a hidden Markov model, and the initial values of the hidden processes $\mathbf{Y}(t)$ must be estimated through Kalman or particle filters. Consequently, to simplify the analysis, we will assume that the processes $\mathbf{Y}(t)$ are either directly observable or obtainable through a filtering approach; however, we will not assume they are tradable.

We now introduce the continuous time counterpart to the discrete model (1a)-(1b) by first defining the Lévy sources of risk $\mathbf{J}(t)$ which drive the market factors $\mathbf{Y}(t)$. Let $\mathbf{J}(t)$ denote a d-dimensional Lévy process with Lévy triple $(\boldsymbol{\gamma}, \boldsymbol{\Sigma}, \boldsymbol{\nu})$ where $\boldsymbol{\gamma}$ represents the vector of drifts, $\boldsymbol{\Sigma}$ represents the variance-covariance matrix of the diffusions, and $\boldsymbol{\nu}$ is the multi-dimensional Lévy density. In this case, the process $\mathbf{J}(t)$ admits the following canonical Lévy-Itô decomposition into its diffusion and jump components (see Sato (1999)):

$$\begin{aligned}
\mathbf{J}(t) &= \boldsymbol{\gamma}\, t + \mathbf{W}(t) + \mathbf{J}^l(t) + \lim_{\epsilon \searrow 0} \mathbf{J}^\epsilon(t) \,, \\
\mathbf{J}^l(t) &= \int_0^t \int_{|\mathbf{Z}| \geq 1} \mathbf{Z}\, \mu(d\mathbf{Z} \times ds) \,, \quad \text{and} \\
\mathbf{J}^\epsilon(t) &= \int_0^t \int_{\epsilon \leq |bZ| < 1} \mathbf{Z}\, \left[\mu(d\mathbf{Z} \times ds) - \nu(d\mathbf{Z} \times ds) \right] \,.
\end{aligned}$$

Here $\mathbf{W}(t)$ is a vector of correlated Brownian motions with covariance matrix $\boldsymbol{\Sigma}$, $\mu(d\mathbf{Z} \times ds)$ is a Poisson random measure counting the number of jumps of size $\mathbf{Z}$ occurring at time s, and $\nu(d\mathbf{Z} \times ds) = \nu(d\mathbf{Z})\, ds$ is its compensator. Note that $\mathbf{J}^l(t)$ and $\mathbf{J}^\epsilon(t)$ carry the interpretation of large and small jumps respectively.

The continuous time counterpart to the discrete model (1a)-(1b) is then defined as follows:

$$d\mathbf{Y}(t) = -\boldsymbol{\kappa}\mathbf{Y}(t_-)dt + d\mathbf{J}(t)\ , \tag{2a}$$

$$\mathbf{X}(t) = \boldsymbol{\theta}(t) + \mathbf{B}\mathbf{Y}(t)\ , \quad \text{and} \tag{2b}$$

$$\mathbf{S}(t) = \mathbf{S}(0)\, e^{\mathbf{X}(t)}\,. \tag{2c}$$

Here, $\boldsymbol{\kappa}$ is a constant matrix, $\boldsymbol{\theta}(t)$ is a deterministic vector, and, without loss of generality[3], the drift of the jump process is set such that the jumps are compensated $\boldsymbol{\gamma}_i = -\int_{\mathbb{R}\setminus\{0\}} z_i\, \nu(dz_i)$. This modeling framework is affine and is similar to that of Duffie, Pan, and Singleton (2000) for modeling interest rates and valuing quanto options among others. However, in that work, the methodology was restricted to valuing European styled claims and required the analytical valuation of the Fourier transform of the payoff function. Here, we consider the framework for commodities, we will not require the transformed payoff analytically, and we will also value path-dependent and earlier exercise options rather easily. The model is also similar to the purely diffusive model of Paschke and Prokopczuk (2008); however, these authors focus on calibrating the model to futures data and do not address option valuation. In addition, Benth, Kallsen, and Meyer-Brandis (2007) introduce a single commodity multi-factor model which is a linear combination of mean-reverting spectrally positive jump processes, each with a different mean-reversion rate, which bears some resemblance to our model. However, our modeling paradigm is more general, contains multiple commodities and we develop an efficient framework for valuing path dependent options. Model (2) should be understood as a model under the real-world probability measure $\mathbb{P}$. Later on we will introduce a class of risk-neutral measures $\mathcal{Q}$ which preserves the real-world structure for the purpose of futures and options valuation.

Before moving onto the valuation issues, we explore a few specific examples to illustrate the flexibility of this modeling framework.

Example 1: *Mean-reverting jump-diffusion.*

Take $d = n = 1$, $\boldsymbol{\theta}(t) = \theta$, $\boldsymbol{\kappa} = \kappa$, $\boldsymbol{\Sigma} = \sigma^2$, $\nu(d\mathbf{Z}) = 0$ and $\mathbf{B} = 1$. This corresponds to the Gibson and Schwartz (1990) one-factor mean-reverting model:

$$d\ln S(t) = \kappa(\theta - \ln S(t))\, dt + \sigma\, dW(t)\ . \tag{3}$$

Also, by letting $\nu(d\mathbf{Z}) = \lambda\, dF(z)$, where F is the normal distribution function, we obtain the Clewlow and Strickland (2000) model:

$$d\ln S(t) = \kappa(\theta - \ln S(t))\, dt + \sigma\, dW(t)\ + dJ(t). \tag{4}$$

[3]The mean-level of $\mathbf{X}(t)$ is fixed by both $\boldsymbol{\gamma}$ and $\boldsymbol{\theta}$, as such, there is a degeneracy which can be removed by either fixing $\boldsymbol{\theta}$ or $\boldsymbol{\gamma}$. Fixing $\boldsymbol{\gamma}$ provides simpler interpretations.

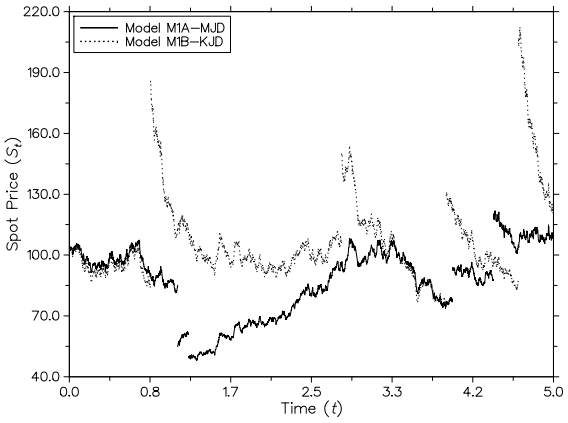

Figure 1. Sample paths of models M1A-MJD (mean-reverting Merton jump-diffusion model) and M1B-KJD (mean-reverting Kou jump-diffusion model) – see Section 4 Example 1 for the specific model parameters.

Further, Cartea and Figueroa (2005) show how to use the Clewlow and Strickland (2000) model for forward prices when the $F(z)$ is arbitrary (up to some technical restrictions). See Figure 1 for sample paths of models M1A-MJD and M1B-KJD – two specific models with parameters reported in Section 4 Example 1 – using the same Brownian increments at each time-step. Notice the large upward jumps and high mean-reversion of *M1B-KJD* model.

Example 2: *Decoupled mean-reverting diffusions and jumps.*

Take $d = 2$, $n = 1$,

$$\boldsymbol{\theta}(t) = \begin{pmatrix} \theta \end{pmatrix} \ , \quad \boldsymbol{\kappa} = \begin{pmatrix} \alpha & 0 \\ 0 & \beta \end{pmatrix} \ , \quad \boldsymbol{\Sigma} = \begin{pmatrix} \sigma^2 & 0 \\ 0 & 0 \end{pmatrix} \ , \quad \mathbf{B} = \begin{pmatrix} 1 & 1 \end{pmatrix} \ , \tag{5}$$

and $\nu(dZ_1 \times dZ_2) = \lambda\, \delta_{Z_1}\, dF(Z_2)$ where δ_z denotes the Dirac measure at 0 and $F(z)$ is a distribution function. This model corresponds to a mean-reverting jump-diffusion with different decay rates for the jumps and diffusion. In particular, log-prices mean-revert to level θ at a rate of α and volatility of σ; while, jumps arrive at a rate of λ, causing log-prices to jump with distribution function $F(z)$, and revert back to zero at a rate of β. This model

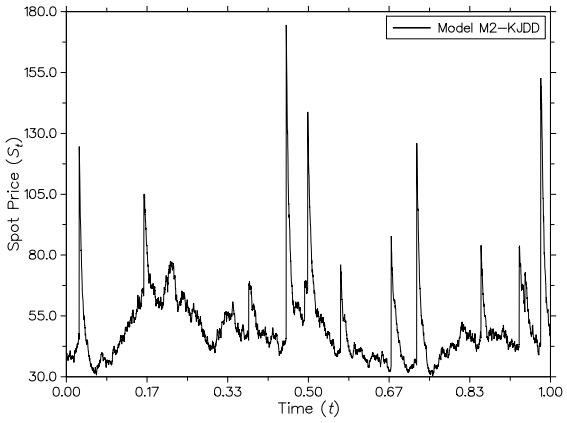

Figure 2. Sample path of M2-KJDD (mean-reverting with double-exponential jumps and decoupled diffusion) – see Section 4 Example 2 for the specific model parameters.

can be rewritten succinctly as

$$\ln S(t) = Y_1(t) + Y_2(t) \,, \tag{6}$$

$$dY_1(t) = \alpha(\theta - Y_1(t))\, dt + \sigma\, dW(t) \,, \tag{7}$$

$$dY_2(t) = -\beta\, Y_2(t)\, dt + dJ(t) \,, \quad \text{and} \tag{8}$$

$$J(t) = \sum_{n=1}^{N(t)} j_n \,. \tag{9}$$

Here, $j_1, j_2, \ldots$ are *iid* with distribution function $F(z)$ and $N(t)$ is a Poisson process with activity λ. This model was proposed in Hikspoors and Jaimungal (2007) and in arithmetic form with spectrally positive jumps in Benth, Kallsen, and Meyer-Brandis (2007). It is particularly well suited for electricity pricing as spikes are typically pulled back much faster than the diffusion components. A similar model is also proposed in Cartea and González-Pedraz (2010) for electricity prices as well as spreads in prices for valuing an electricity interconnector between countries.

In Figure 2, a sample path of model *M2-KJDD* – a specific model with parameters provided in Section 4 Example 2 – is shown . Notice the extreme spikes and their quick reversion to the mean, common in electricity markets. However, the relatively low mean-reversion of the diffusion term allows for non-trivial diffusion structure.

Example 3: *Co-dependent jumps and correlated diffusions.*

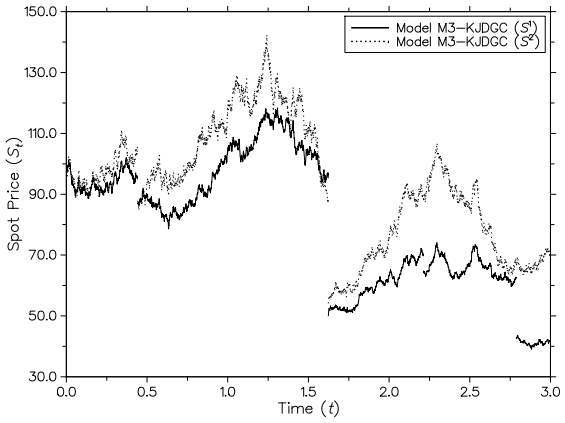

Figure 3. Sample path of model M3-MJDGC (mean-reverting with idiosyncratic jumps and cojoined bivariate Gaussian jumps) – see Section 4 Example 3 for specific model parameters.

Take $d = 2$, $n = 2$,

$$\boldsymbol{\theta} = \begin{pmatrix} \theta \\ \phi \end{pmatrix} , \quad \boldsymbol{\kappa} = \begin{pmatrix} \alpha & 0 \\ 0 & \beta \end{pmatrix} , \quad \boldsymbol{\Sigma} = \begin{pmatrix} \sigma^2 & \rho\sigma\eta \\ \rho\sigma\eta & \eta^2 \end{pmatrix} , \quad \mathbf{B} = \begin{pmatrix} 1 & 0 \\ 0 & 1 \end{pmatrix} , \tag{10}$$

and $\nu(dZ_1 \times dZ_2) = dC(F_1(Z_1), F_2(Z_2))$ with $C(u, v)$ a copula and $F_i(z)$ two marginal distribution functions. This is a new model class and corresponds to a two-dimensional jump-diffusion where the diffusions are correlated, and jumps may have co-dependent pieces. It is the presence of the copula function here which allows for in general co-dependent jumps as well as independent jumps. This model can be used when two commodities are strongly dependent; however, it will allow for jumps in one price without necessitating a jump in the other. See Figure 3 for a typical sample path of model M3-MJDGC – a specific model with parameters reported in Section 4 Example 3. Notice the co-dependent structure of jumps in the two dimensions. As previously mentioned, the model is flexible enough to allow for independent jumps (see $t \approx 2.75$) and simultaneous jumps (see $t \approx 1.6$).

Example 4: *Mean-reverting to a mean-reverting level.*

Take $d = 2$, $n = 1$,

$$\boldsymbol{\theta}(t) = \begin{pmatrix} \theta \end{pmatrix} , \quad \boldsymbol{\kappa} = \begin{pmatrix} \alpha & -\alpha \\ 0 & \beta \end{pmatrix} , \quad \boldsymbol{\Sigma} = \begin{pmatrix} \sigma^2 & \rho\sigma\eta \\ \rho\sigma\eta & \eta^2 \end{pmatrix} , \quad \mathbf{B} = \begin{pmatrix} 1 & 0 \end{pmatrix} , \tag{11}$$

and $\nu(dZ_1 \times dZ_2) = 0$. This corresponds to a two factor mean-reverting model. In this case, the log-prices mean-revert to a stochastic long-run mean which itself mean-reverts to a fixed

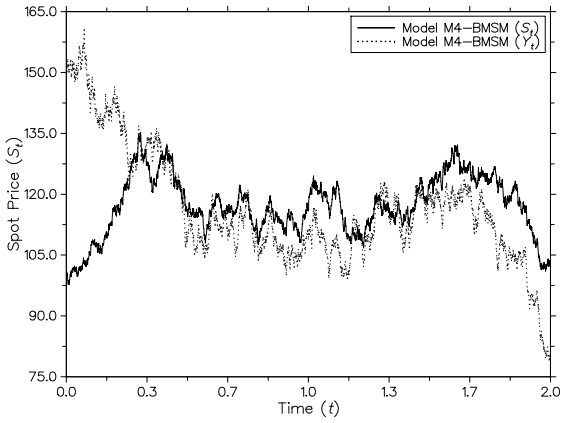

Figure 4. Sample path of model M4-BMSM (mean-reverting to a mean-reverting long run level) – see Section 4 Example 4 for specific model parameters.

level and can be rewritten as

$$d\ln S(t) = \alpha(\Upsilon(t) - \ln S(t))dt + \sigma\, dW_1(t)\,, \quad \text{and} \tag{12}$$

$$d\Upsilon(t) = \beta(\theta - \Upsilon(t))dt + \eta\, dW_2(t)\ . \tag{13}$$

See Figure 4 for a typical sample path of model M4-BMSM – with parameters as specified in Section 4 Example 4. Notice how the spot price process $S(t)$ reverts to the stochastic mean process $\exp\{\Upsilon(t)\}$.

This model, similar to the stochastic convenience yield model of Schwartz (1997) and the two-factor model of Schwartz and Smith (2000), was introduced in Barlow, Gusev, and Lai (2004) where the authors developed Kalman filter estimates for the hidden stochastic long run mean process $\Upsilon(t)$. The authors then fitted the model parameters to electricity price data. They found that the fit was not very good – this is no surprise as there are no spikes in (12)-(13), while electricity data are known to have notoriously large spikes. On the other hand, the model is further analyzed in Hikspoors and Jaimungal (2007) in context of derivative valuation where crude oil futures data is used to calibrate the model. In that context, the model was found to be very satisfactory. Jumps can trivially be included by setting the Lévy density ν to the desired one.

Given our general model (2), we first derive an expression for European option prices for all spots using a Fourier transform representation. Then, through this representation, Bermudan, American, barrier and other path dependent options can be valued using a time-stepping adaptation of the Fourier representation which we dub the *mean-reverting Fourier Space Time-Stepping* (mrFST)

algorithm. Note that to value options and/or futures, it is necessary to change probability measures from the real-world to the risk-neutral. Since the market is incomplete, as well as the existence of storage costs (or the impossibility of buy and hold strategies – e.g., with electricity), convenience yields and illiquidity in the market, there are many equivalent risk-neutral measures. In Appendix B we provide a specific class of equivalent measures $\mathcal{Q}$ which preserves the structure of our real-world model (2). Since the structure is preserved we will pick a specific measure $\mathbb{Q} \in \mathcal{Q}$ and choose to use the same labels for the real-world and risk-neutral parameters to save notation. To be clear, it should be understood that from this point onwards all models and parameters are under the risk-neutral measure. With these comments in mind, the main result on which we build our algorithm is provided in Theorem 2.1 below and proven in Appendix C.

Theorem. 2.1 *The price $V(t,\mathbf{y})$ of a European option written on the vector of price processes $\mathbf{S}(t) = \mathbf{S}(0)\, e^{\boldsymbol{\theta}(t)+\mathbf{B}\,\mathbf{Y}(t)}$ with payoff function $\phi(\mathbf{Y}(T)) = \varphi(\mathbf{S}(T))$ is*

$$V(t,\mathbf{y}) = e^{-r(T-t)}\mathcal{F}^{-1}\left[\mathcal{F}[\phi(\mathbf{y})](e^{\boldsymbol{\kappa}'(T-t)}\,\boldsymbol{\omega})\; e^{\Psi(\boldsymbol{\omega},T-t)+(T-t)\mathrm{Tr}\,\boldsymbol{\kappa}}\right](\mathbf{y})\;, \tag{14}$$

where

$$\Psi(\boldsymbol{\omega},s) = \int_0^s \psi(e^{\boldsymbol{\kappa}' u}\,\boldsymbol{\omega})\,du\;, \qquad \textit{and} \tag{15}$$

$$\psi(\boldsymbol{\omega}) = i\boldsymbol{\gamma}'\boldsymbol{\omega} - \tfrac{1}{2}\boldsymbol{\omega}'\boldsymbol{\Sigma}\boldsymbol{\omega} + \int_{\mathbb{R}^d/\{0\}} \left(e^{i\boldsymbol{\omega}'\mathbf{y}} - 1 - i\,\mathbf{1}_{\{|\mathbf{y}|<1\}}\,\boldsymbol{\omega}'\mathbf{y}\right)\nu(d\mathbf{y})\;, \tag{16}$$

$\mathcal{F}[.]$ and $\mathcal{F}^{-1}[.]$ denote the Fourier and inverse Fourier transforms respectively, and $'$ denotes transpose.

Proof. See Appendix C. □

Notice that the function $\psi(\boldsymbol{\omega})$ is the characteristic exponent of the driving Lévy process, while the function $\Psi(\boldsymbol{\omega}, T-t)$ accounts for the mean-reverting nature through the exponential rescaling of frequencies.

The appearance in expression (14) of the scaled frequency of the transform of option prices $\mathcal{F}[\phi(\mathbf{y})](e^{\boldsymbol{\kappa}'(T-t)}\,\boldsymbol{\omega})$ seems to pose problems since, on a discrete grid, this scaling implies *extrapolating* to points in frequency space beyond the grid boundaries. However, by the scaling property of Fourier transforms, it is possible to obtain these values from *interpolated* option prices in real space:

$$\mathcal{F}[\phi](e^{\boldsymbol{\kappa}'(T-t)}\,\boldsymbol{\omega}) = \mathcal{F}[\breve{\phi}](\boldsymbol{\omega})\, e^{-(T-t)\,\mathrm{Tr}\boldsymbol{\kappa}}\;, \tag{17}$$

where $\breve{\phi}(\mathbf{y}) \triangleq \phi(\mathbf{y}\, e^{-(T-t)\kappa'})$. Collecting the above with equation (14) provides an alternate repre-

sentation for European option prices

$$v(t,\mathbf{y}) = \mathcal{F}^{-1}\left[\mathcal{F}[\breve{\phi}(\mathbf{y})](\boldsymbol{\omega})\, e^{\Psi(\boldsymbol{\omega},T-t)}\right](\mathbf{y})\,. \tag{18}$$

This rewriting appears rather trivial, however, it immensely reduces the complexity of the method by shifting the attention from high frequency modes, which requires *extrapolating* the transformed prices, to small scales in the spatial directions, which requires *interpolating* the prices. This representation will be used in the derivation of the time-stepping method in the next section.

Many commodity derivatives are written solely on the forward prices (or futures prices – which in the deterministic interest rate environments are identical). For example, consider valuing an oil field in which oil is extracted through a number of years. Assuming extraction occurs at an exponentially decaying rate $\alpha e^{-\beta t}$, the value of the future cash-flow can represented as

$$V_t = \mathbb{E}_t^{\mathbb{Q}}\left[\int_t^T \alpha e^{-\beta u}\, S_u\, du\right] = \int_t^T \alpha^{-\beta u}\, F_t(u)\, du\,,$$

where $F_t(u)$ is the futures price of maturity u viewed at time t. If an investor has the option to start extracting the field at any time, it can be viewed as an American Asian option on the futures contract. Consequently, it is prudent to investigate futures prices in our model. In this case, forward prices follow as an easy consequence of Theorem 2.1.

Corollary 2.2 *The T-maturity forward prices $\{F_1(t,T),\ldots,F_n(t,T)\}$ based on the spot price model (2) are*

$$\mathbf{F}_i(t,T) = \exp\left\{\theta_i(T) + \Psi(-i\, e^{-\boldsymbol{\kappa}'(T-t)}\mathbf{b}_i,\, T-t) + e^{-\boldsymbol{\kappa}'(T-t)}\mathbf{b}_i\mathbf{Y}(t)\right\}\,, \tag{19}$$

where, $(\mathbf{b}_i)_j = \mathbf{B}_{ij}$.

Proof. A simple application of Theorem 2.1 with payoff function $\phi_i(\mathbf{y}) = \mathbf{S}(0)\exp\{\boldsymbol{\theta}(T) + \mathbf{B}\,\mathbf{y}\}$ provides the result. □

This result shows that the futures prices can be rewritten in terms of the market factors $\mathbf{Y}_t$ and is particularly useful when valuing options on a strip of futures – such as the option to invest in an oil field described above. Consequently, only the market factors have to be modeled, rather than the entire futures curve, and options can be valued by propagating prices as a function of $\mathbf{Y}$ backwards and then translating to futures prices.

In the next section we demonstrate how Theorem 2.1 can be used to value early exercise options recursively through a time-stepping algorithm.

3. Mean-Reverting Fourier Space Time-Stepping Algorithm

We now develop a time-stepping algorithm for valuing early exercise features such as those appearing in Bermudan, American and swing style contingent claims. To this end, let $\Omega = [-\mathbf{y}^{min}, \mathbf{y}^{max}]$ be a finite d-dimensional discrete space domain with N^d uniformly spaced points. The discretization of the frequency domain is then fixed as $\hat{\Omega} = [0, \boldsymbol{\omega}^{\max}]$, with the Nyquist condition $\Delta\mathbf{y} \cdot \Delta\boldsymbol{\omega} = 1/N$ being satisfied in each dimension. Numerical experiments show that choosing $\mathbf{y}^{\min}, \mathbf{y}^{\max} \in [4, 7]$ provides accurate results for the options and commodity price models considered in this work, although, for price processes having large spikes, larger values may be needed. Let $t = t_0, t_1, \ldots, t_M = T$, $\Delta t_m = t_m - t_{m-1}$ be a discretization of the time domain into M intervals and let $\mathbf{v}_m$ denote the discrete array of option values at time t_m.

The pricing equation (18) provides values for a full spectrum of spot prices. Replacing the continuous Fourier transform with discrete Fourier transforms, which in turn are computed using the fast Fourier transform (FFT) algorithm, leads to the mean-reverting Fourier-space time stepping (mrFST) algorithm for propagating a price one time-step back:

$$\mathbf{v}_{m-1} = \mathsf{FFT}^{-1}\left[\mathsf{FFT}[\breve{\mathbf{v}}_m](\boldsymbol{\omega})\; e^{\Psi(\boldsymbol{\omega},\Delta t_m)}\right] . \tag{20}$$

Here, $\breve{\mathbf{v}}_m$ represents the spatial rescaling of $\mathbf{v}_m$, specifically $\breve{\mathbf{v}}_m(\mathbf{y}) \triangleq \mathbf{v}_m(\mathbf{y}\, e^{-(T-t)\kappa'})$.

European options can be priced using a single time step ($\Delta t = T - t$) of the mrFST method. Thus, two evaluations of the FFT algorithm and one scaling operation provides option prices for a range of spot prices. The mrFST algorithm can also be used to value Bermudan styled claims by taking multiple time-steps and enforcing the optimal exercise condition explicitly as follows

$$\mathbf{v}_{m-1} = \max\left\{\mathsf{FFT}^{-1}\left[\mathsf{FFT}[\breve{\mathbf{v}}_m](\boldsymbol{\omega})\; e^{\Psi(\boldsymbol{\omega},\Delta t_m)}\right] , \mathbf{I}_{m-1}\right\} , \tag{21}$$

where $\mathbf{I}_{m-1}$ is the intrinsic (or exercise) value of the option at time step $m-1$. Alternatively, a penalty method, as developed in Jackson, Jaimungal, and Surkov (2008), could be used. Barrier options can be priced similarly by enforcing appropriate barrier conditions

$$\mathbf{v}_{m-1} = \mathsf{FFT}^{-1}\left[\mathsf{FFT}[\breve{\mathbf{v}}_m](\boldsymbol{\omega})\; e^{\Psi(\boldsymbol{\omega},\Delta t_m)}\right] \cdot \mathbb{1}_{\{\boldsymbol{\theta}+\mathbf{B}\overline{\mathbf{Y}}<B\}} + R \cdot \mathbb{1}_{\{\boldsymbol{\theta}+\mathbf{B}\overline{\mathbf{Y}}\geq B\}} , \tag{22}$$

where R is the rebate being paid upon crossing of the barrier B.

When there is no closed form expression for the characteristic function, the computation of $\Psi(\boldsymbol{\omega}, \Delta t_m)$ can become time expensive. However, different contracts on the same underlier will require the same characteristic function; consequently, $e^{\Psi(\boldsymbol{\omega},\Delta t_m)}$ should be precomputed and stored both for the valuation of path-dependent options, where the cardinality of the set $\{\Delta t_i\}$ is typically small, and for the valuation of a book of European options simultaneously.

Below we provide the characteristic functions for the four examples studied in this paper and discuss some associated computational aspects.

Example 1: *Mean-reverting jump-diffusion model* (4).

$$\Psi(\omega, \Delta t) = -\frac{\omega^2\sigma^2}{4\kappa}(e^{2\kappa\Delta t} - 1) + \int_0^{\Delta t} \widehat{\psi}(e^{\kappa u}\omega)du \tag{23}$$

where

$$\widehat{\psi}(\omega) = \int_{-\infty}^{\infty} (e^{i\omega y} - 1)dF(y)\,, \tag{24}$$

is the characteristic function of the jumps in (16) and $F(y)$ is the distribution function of the jumps. For the Kou (2002) jump-diffusion model, in which jumps are double exponentially distributed,

$$\widehat{\psi}(\omega) = \lambda\left\{\frac{p}{1 - i\omega\eta_+} + \frac{1-p}{1 + i\omega\eta_-} - 1\right\}\,,$$

and the integral can be computed analytically as follows

$$\int_0^{\Delta t} \widehat{\psi}(e^{\kappa u}\omega)du = \frac{\lambda}{\kappa}\left(p\ln h(\omega, \eta_+) + (1-p)\ln h(\omega, -\eta_-) - \kappa\Delta t\right), \tag{25}$$

where

$$h(\omega, \eta) = \frac{1 - i\omega\eta}{e^{-\kappa\Delta t} - i\omega\eta}\,.$$

For the Merton (1976) jump diffusion model, in which jumps are normally distributed with mean $\tilde{\mu}$ and variance $\tilde{\sigma}^2$,

$$\widehat{\psi}(\omega) = \lambda\left\{e^{i\tilde{\mu}\omega - \frac{1}{2}\tilde{\sigma}^2\omega^2} - 1\right\}\,,$$

and the integral must be approximated numerically

$$\int_0^{\Delta t} \widehat{\psi}(e^{\kappa u}\omega)du \approx \sum_{p=0}^{P} \zeta_p \widehat{\psi}(e^{\kappa u_p}\omega). \tag{26}$$

In the above expressions, u_p and ζ_p are the appropriate nodes and weights determined by the chosen quadrature rule and the number of subintervals P. For comparison purposes, we computed the integral for the Kou model and found that for all ω it can be computed within

an absolute error tolerance level of 10^{-3} by using a composite Simpson rule with 7 subintervals (and 9 subintervals for absolute error tolerance level of 10^{-4}). Choosing a larger number of subintervals had no significant effect on the resulting option prices in the numerical examples studied here.

Example 2: *Decoupled mean-reverting diffusion and jump model* (6)-(9).

$$\Psi(\omega_1, \omega_2, \Delta t) = -\frac{\omega_1^2 \sigma^2}{4\alpha}(e^{2\alpha\Delta t} - 1) + \int_0^{\Delta t} \widehat{\psi}(e^{\beta u}\omega_2) du. \tag{27}$$

The integral term, again, depends on the jump distribution and is computed in the same fashion as in Example 1. Notice that the first term above contains only the frequencies ω_1, while the integral term contains only the frequencies ω_2. This factorization is a direct consequence of the decoupling between the diffusive and jump terms in this model.

Example 3: *Co-dependent jumps and correlated diffusions model* (10).

$$\begin{aligned}\Psi(\boldsymbol{\omega}, \Delta t) = &-\frac{\omega_1^2 \sigma_1^2}{4\alpha}(e^{2\alpha\Delta t} - 1) - \frac{\omega_2^2 \sigma_2^2}{4\beta}(e^{2\beta\Delta t} - 1) - \rho\omega_1\omega_2\sigma_1\sigma_2 \frac{e^{(\alpha+\beta)\Delta t} - 1}{\alpha + \beta} \\ &+ \int_0^{\Delta t} \widehat{\psi}_1(e^{\alpha u}\omega_1) du + \int_0^{\Delta t} \widehat{\psi}_2(e^{\beta u}\omega_2) du + \int_0^{\Delta t} \widetilde{\psi}(e^{\boldsymbol{\kappa}' u}\boldsymbol{\omega}, \Delta t)\, du\ .\end{aligned} \tag{28}$$

Here, $\widehat{\psi}_1$ and $\widehat{\psi}_2$ are the characteristic functions of the idiosyncratic jumps (as in (24)), and $\widetilde{\psi}(\boldsymbol{\omega}, \Delta t)$ is the characteristic function of the codependent jumps:

$$\widetilde{\psi}(\boldsymbol{\omega}, \Delta t) = \widetilde{\lambda}\left[\int_{\mathbb{R}^2} e^{i(x_1\omega_1 + x_2\omega_2)} f_1(x_1) f_2(x_2) c(F_1(x_1), F_2(x_2)) dx_1 dx_2 - 1\right]\ , \tag{29}$$

with, $f_{1,2}$, F and c being the marginal probability, cumulative probability and copula density functions respectively, and $\widetilde{\lambda}$ is the arrival rate of codependent jumps. The first two integrals in equation (28) are computed in the same manner as in Example 1, while the computation of the last integral depends on the chosen copula and marginal densities. For the special case of a Gaussian copula, with parameter $\widetilde{\rho}$, and the marginal distribution of jumps normal with means $\widetilde{\mu}_{1,2}$ and variances $\widetilde{\sigma}_{1,2}^2$, the co-dependent jump becomes a bivariate Guassian and $\widetilde{\psi}$ is easily computed to be

$$\widetilde{\psi}(\boldsymbol{\omega}, \Delta t) = \widetilde{\lambda}\left(\exp\left\{i\widetilde{\mu}_1\omega_1 + i\widetilde{\mu}_2\omega_2 - \tfrac{1}{2}\widetilde{\sigma}_1^2\omega_1^2 - \widetilde{\rho}\widetilde{\sigma}_1\widetilde{\sigma}_2\omega_1\omega_2 - \tfrac{1}{2}\widetilde{\sigma}_2^2\omega_2^2\right\} - 1\right). \tag{30}$$

For other cases, such as a Clayton copula or double-exponential marginals, the copula characteristic function (29) has to be approximated numerically. In principle, any discretization scheme can be used since (29) can be computed once and stored for future use in the time-

stepping algorithm. We are currently developing an efficient FFT-based approach for computing such two-dimensional integrals, extending the approach of computing Fourier integrals using the FFT outlined in Press, Teukolsky, Vetterling, and Flannery (1992).

Example 4: *Mean-reverting to a mean-reverting level* (12)-(13).

$$\Psi(\omega, \Delta t) = -\tfrac{1}{2}\boldsymbol{\omega}'\widetilde{\boldsymbol{\Sigma}}(\Delta t)\boldsymbol{\omega}, \tag{31}$$

where

$$\widetilde{\boldsymbol{\Sigma}}(s) \triangleq \boldsymbol{\Gamma}'\widehat{\boldsymbol{\Sigma}}(s)\boldsymbol{\Gamma}\,, \qquad (\widehat{\boldsymbol{\Sigma}}(s))_{ij} = \frac{e^{(\lambda_i+\lambda_j)s}-1}{\lambda_i+\lambda_j}(\boldsymbol{\Gamma}\boldsymbol{\Sigma}\boldsymbol{\Gamma}')_{ij}\,,$$

and $\boldsymbol{\Gamma}$ is the matrix of orthonormalized eignevectors of $\boldsymbol{\kappa}$ stacked columnwise with eigenvalues $\{\lambda_1, \ldots, \lambda_d\}$.

4. Numerical Results and Applications

In this section, we present several numerical experiments to investigate the convergence and precision of the mrFST method. Specifically, we probe the pricing of single-asset European, American and discrete barrier options, and multi-asset European and Bermudan spread options, under the four example spot price processes described in Section 2. Swing options are discussed afterwards in Section 5.

Example 1: *Mean-reverting jump-diffusion model* (4). In this example, two models are used in the pricing experiments. The first model, which we refer to as *M1A-MJD*, has log-normal jumps (mean-reverting extension of the Merton (1976) jump-diffusion model as in Clewlow and Strickland (2000)) and parameters $\sigma = 0.2, \lambda = 1.0, \widetilde{\mu} = -0.1, \widetilde{\sigma} = 0.25, \theta = 90.0, \kappa = 0.75, r = 0.05$. The second model, which we refer to as *M1B-KJD*, has double-exponential jumps (mean-reverting extension of the Kou (2002) jump-diffusion model) and parameters $\sigma = 0.25, \lambda = 0.6, p = 0.95, \eta_+ = 0.45, \eta_- = 0.35, \theta = 92.0, \kappa = 3.5, r = 0.06$. Figure 1 shows sample paths of both models using the same Brownian increments at each time-step. Notice the large upward jumps and high mean-reversion of *M1B-KJD* model.

For each of the two models we price three options: (i) European and (ii) American put option with parameters $S = 100$, $K = 105$, $T = 1$, which we refer to as *O1A-EUR* and *O1B-AMR* respectively; (iii) a discretely monitored barrier down-and-out put option with daily monitoring and parameters $S = 100$, $K = 105$, $T = 1$, $B = 90$, $R = 3$, which we refer to as *O1C-DBR*.

Pricing the *O1A-EUR* option under *M1A-MJD* model requires a single time-step, as outlined in Section 3. Under the *M1B-KJD* model, however, we split the pricing interval $[0, T]$ into 8 equal

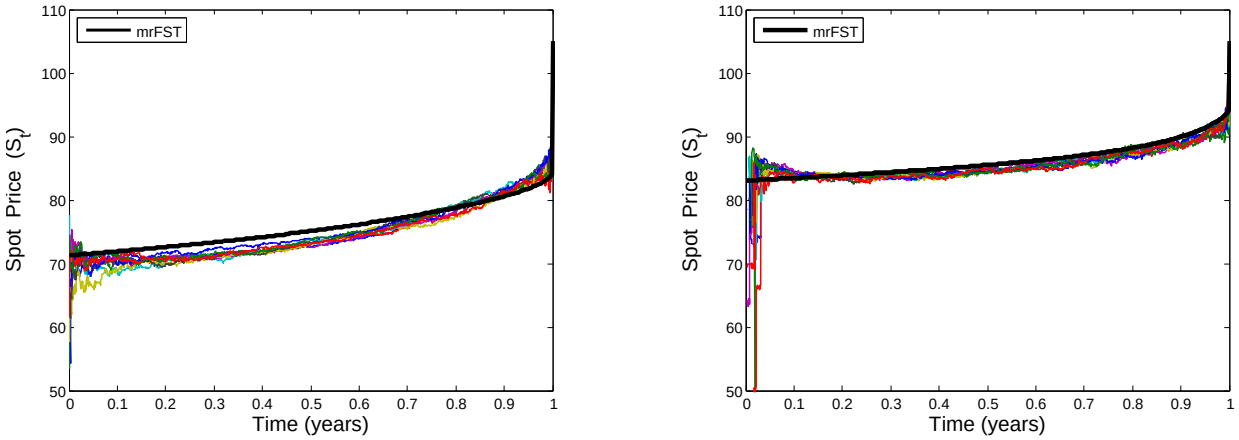

(a) M1A-MJD (b) M1B-KJD

Figure 5. Optimal exercise boundaries for the O1B-AMR option under the Merton (M1A-MJD) and Kou (M1B-KJD) jump-diffusion models. The solid smooth curve is the result of the mrFST method. The other curves are the optimal exercise curves from 10 separate replications of LSMC simulations. Notice that the LSMC curves are clearly suboptimal, noisy and the prices (reported in Tables 3 and 4) are biased downward.

time-steps. This is due to the fact $e^{-\kappa T} \approx 0.03$ which causes very large scaling of the payoff function. By taking 8 time-steps we reduce the scaling to $e^{-\kappa \Delta t} \approx 0.88$. In general, when pricing European options, we chose the number of time-steps to be $\lceil 2\kappa T \rceil$ to reduce the effect of extreme scaling. We find that the mrFST method attains second order convergence in space when pricing European options, as shown in Tables 1 and 2.

When pricing the *O1B-AMR* option we take small time-steps to monitor exercise behaviour and therefore the scaling at each time step is small. By applying Richardson extrapolation, the mrFST method attains second order convergence in time for pricing of American options, as shown in Tables 3 and 4. For comparison purposes, in Figure 5, we show the optimal exercise boundaries found via a least squares Monte Carlo simulation (à la Carriere (1996) and Longstaff and Schwartz (2001)) in comparison to the mrFST method. 100,000 sample paths were used for each optimal exercise curve. The figure shows ten such curves from ten replications of the simulations. These replications were also used to obtain the price confidence intervals reported in Tables 3 and 4. It is well known that the LSMC method produces suboptimal exercise curves and undervalues the option – as we have found here. Nonetheless, the resulting boundaries and prices are comparable. There is a clear advantage for the mrFST method over the LSMC in terms of both computational time and accuracy of the optimal of exercise boundaries as can be seen from the simulation errors in Figure 5.

For pricing *O1C-DBR* options, the time-steps are set equal to the interval between monitoring dates – for the specific contract valued here, 1 year maturity with daily exercise, 252 time-steps are required (equivalent to 252 trading days in a year). Weekends and holidays can also be accounted for by varying Δt at various time-steps. The mrFST method has first order convergence in space for pricing of *O1C-DBR* option, as shown in Tables 5 and 6.

Example 2: *Decoupled mean-reverting diffusion and jump model* (6)-(9). The chosen model parameters are

$$\boldsymbol{\theta} = \begin{pmatrix} 50 \end{pmatrix}, \quad \boldsymbol{\kappa} = \begin{pmatrix} 7.5 & 0 \\ 0 & 100 \end{pmatrix}, \quad \boldsymbol{\Sigma} = \begin{pmatrix} 1.0 & 0 \\ 0 & 0 \end{pmatrix}, \quad \mathbf{B} = \begin{pmatrix} 1 & 1 \end{pmatrix}, \tag{32}$$

$r = 0.05$ and $\nu(d\mathbf{Z}) = \lambda dF(z_2)$ where $\lambda = 20.0$ and F is the double exponential cdf with parameters $p = 0.99, \eta_+ = 0.4, \eta_- = 0.05$. We refer to this model as *M2-KJDD*. Figure 2 provides a sample path for this model. Notice the extreme spikes and their quick reversion to the mean, common in electricity markets. However, the relatively low mean-reversion of the diffusion term allows for non-trivial diffusion structure. Under this model, we price European (model *O2-EUR*) and daily exercisable Bermudan (model *O2-BRM*) call options with parameters $S = 40$, $K = 42$, $T = 0.25$.

The mrFST method has second order convergence in space for both European and Bermudan options, as reported in Tables 7 and 8. Since the problems are two dimensional, the computations are significantly slower than those in Example 1. For the *O2-EUR* option, 16 time-steps are taken to reduce the scaling required by the mrFST method. For the *O2-BRM* option, 63 time-steps are taken (1 step per day) since the contract allows for daily exercise during the 3 month life of the option.

Example 3: *Co-dependent jumps and correlated diffusions model* (10). The chosen parameters for the model are

$$\boldsymbol{\theta} = \begin{pmatrix} 92 \\ 110 \end{pmatrix}, \ \boldsymbol{\kappa} = \begin{pmatrix} 0.5 & 0 \\ 0 & 0.75 \end{pmatrix}, \ \boldsymbol{\Sigma} = \begin{pmatrix} 0.2^2 & 0.7 \cdot 0.06 \\ 0.7 \cdot 0.06 & 0.3^2 \end{pmatrix}, \ \mathbf{B} = \begin{pmatrix} 1 & 0 \\ 0 & 1 \end{pmatrix}, \tag{33}$$

$r = 0.05$, and $\nu(d\mathbf{Z}) = \lambda_1 dF_1(z_1) d(\mathbb{I}_{z_2>0}) + \lambda_2 d(\mathbb{I}_{z_1>0}) dF_2(z_2) + \widetilde{\lambda} dC(F_1^\star(z_1), F_2^\star(z_2))$. The idiosyncratic jumps were chosen as follows: $\lambda^1 = 0.75$, $p^1 = 0.45$, $\eta_+^1 = 0.25$, $\eta_-^1 = 0.125$, $\lambda^2 = 0.5$, $p^2 = 0.55$, $\eta_+^2 = 0.3$, $\eta_-^2 = 0.2$. The copula jumps are driven by a Gaussian copula with correlation parameter 0.7 and have arrival rate of $\widetilde{\lambda} = 1.0$. The copula jumps have normal distribution with means $-0.1, 0.1$ and variances $0.2^2, 0.3^2$ respectively. Alternatively, one can view the jumps as being drawn from a bivariate Gaussian distribution with mean $(-0.1; 0.1)$ and covariance matrix $[0.2^2,\ 0.042\ ;\ 0.042,\ 0.3^2]$. We refer to the model as *M3-MJDGC*. Figure 3 illustrates a sample path

from the model. Notice the co-dependent structure of jumps in the two dimensions. As previously mentioned, the model is flexible enough to allow for independent jumps (see $t \approx 2.75$) and simultaneous jumps (see $t \approx 1.6$). Under this model, we price European and Bermudan (monthly exercise) spread call options with parameters $S_1 = 100$, $S_2 = 100$, $K = 3.5$, $T = 1$. We refer to these option as *O3-ESPD* and *O3-BSPD* respectively.

Tables 9 and 10 demonstrate that the mrFST attains second order convergence for European and Bermudan multi-asset options. For the *O3-ESPD* option, 2 time steps are taken to reduce the effect of scaling. For the *O3-BSPD* option, 12 time-steps are required as the option can only be exercised 12 times during its life.

Example 4: *Mean-reverting to a mean-reverting level* (12)-(13). The chosen model parameters are

$$\boldsymbol{\theta} = \begin{pmatrix} 100 \end{pmatrix}, \ \boldsymbol{\kappa} = \begin{pmatrix} 2.5 & -2.5 \\ 0 & 1.0 \end{pmatrix}, \ \boldsymbol{\Sigma} = \begin{pmatrix} 0.2^2 & 0.5 \cdot 0.06 \\ 0.5 \cdot 0.06 & 0.3^2 \end{pmatrix}, \ \mathbf{B} = \begin{pmatrix} 1 & 0 \end{pmatrix}, \tag{34}$$

and $r = 0.04$. We refer to this model as *M4-BMSM* and provide a sample path under this model in Figure 4. As expected, the spot price process $S(t)$ reverts to the stochastic mean process $\exp\{\Upsilon(t)\}$. Under this model we price a European call option with parameters $S = 100$, $K = 100$, $T = 2.0$, which we refer to as *O4-EUR*.

Based on the results in Table 11, the mrFST method has second order convergence in space. Note, that 4 time-steps are required to reduce the effect of extreme scaling. While a closed-form solution exists for the *O4-EUR* option under *M4-BMSM* model, no such simplification occurs for path dependent options. Nonetheless, the mrFST method allows us to price path-dependent options efficiently.

5. Valuation of Swing Options

As previously mentioned, swing options are quite common in electricity and natural gas markets. Swing options provide constrained flexibility with respect to volume and timing of energy delivery. As an example, consider the following contract: The holder of the option agrees to purchase $100MWh$ at a cost of $\$45/MWh$ over a period of 1 month. At the start of each hour, the holder has the right to increase power consumption to $110MW$ for that hour (swing up) or decrease to $90MW$ (swing down) at the same price. The total number of such changes is limited to 50. There are two essential components to the swing option: a pure forward agreement to deliver a fixed amount of energy over a period of time and the variational or "swing" component, which is the right to change consumption at the option holder's choosing.

To formalize the discussion, let $V_m(\mathbf{X}, Q)$ denote the value of the swing option at time t_m having

exercised the right to change consumption Q times prior. At each 'swing' opportunity, the holder has a choice to change their consumption q times (or by q units). The cash-flow function Φ_m captures the immediate monetary benefit of such a change in consumption at time t_m. For instance, the extra supply may be sold into the market when energy prices are high. Thus, it is possible to express the value of the swing option as solution to the following dynamic programming equation:

$$V_{m-1}(\mathbf{X}, Q) = \max_q \left\{ \Phi_{m-1}(\mathbf{X}, q) + e^{-r\Delta t}\mathbb{E}[V_m(\mathbf{X}, Q+q)] \right\} . \tag{35}$$

The choices available to the option holder are: do nothing ($q = 0$), increase consumption, or swing up ($q > 0$) and decrease consumption, or swing down ($q < 0$). The amount of consumption changes may be bounded $|Q_m| \leq \overline{Q}$ either in relative terms $Q_m = \sum_{j=1}^m q_j$ or absolute terms $Q_m = \sum_{j=1}^m |q_j|$. The cashflow function $\Phi(\mathbf{X}, q)$ may include a penalty term to enforce additional limits on Q, or may be as simple as the value of selling the extra supply into the market $\Phi(\mathbf{X}, q) = q(e^{\mathbf{X}} - K)$.

While the structure of the dynamic programming equation may be slightly different for more exotic types of swing contracts, the critical part of the algorithm is the computation of the expectation in equation (35). We propose to use the mrFST method to carry out that essential computation. By using the mrFST method, one can easily incorporate jumps, and, if two commodities are tied together in the swing contract, co-dependence. Furthermore, there is a huge efficiency and accuracy gain over traditional Monte Carlo methods or multi-node forest methods (stacks of trees). For the mrFST method, as in all other methods, one requires keeping a stack of option values $V(\cdot, Q)$ for differing levels of total consumption. These prices are then propagated back in time using the mrFST algorithm. Furthermore, forward and backward FFT transforms can be applied efficiently to the entire stack by utilizing the multi-data FFT transform available in most FFT packages (multi-core architectures can be especially effective for such applications).

Figure 6 depicts the effect of changing mean reversion speed κ on the value of a swing option. The option parameters are $S = 100$, $K = 100$, $T = 2$, $-3 \leq Q \leq 5$ (number of swings being bounded in relative terms) and the commodity price model is mean-reverting Merton jump-diffusion $\sigma = 0.75, \lambda = 0.5, \widetilde{\mu} = 0.1, \widetilde{\sigma} = 0.2, r = 0.05$. Generally, higher mean-reversion causes less volatility in the spot price, making the swing option less valuable. When spot price is small, however, higher mean reversion increases swing value, as there is higher probability of spot price rising significantly above the strike price during the life of the option.

6. Conclusions

In this article we introduce a new multi-factor cross-commodity model which incorporates jumps and cointegration in prices. The formulation is quite flexible, and a number of important commodity models arise as special cases of our model. Furthermore, we develop a new robust and flexible

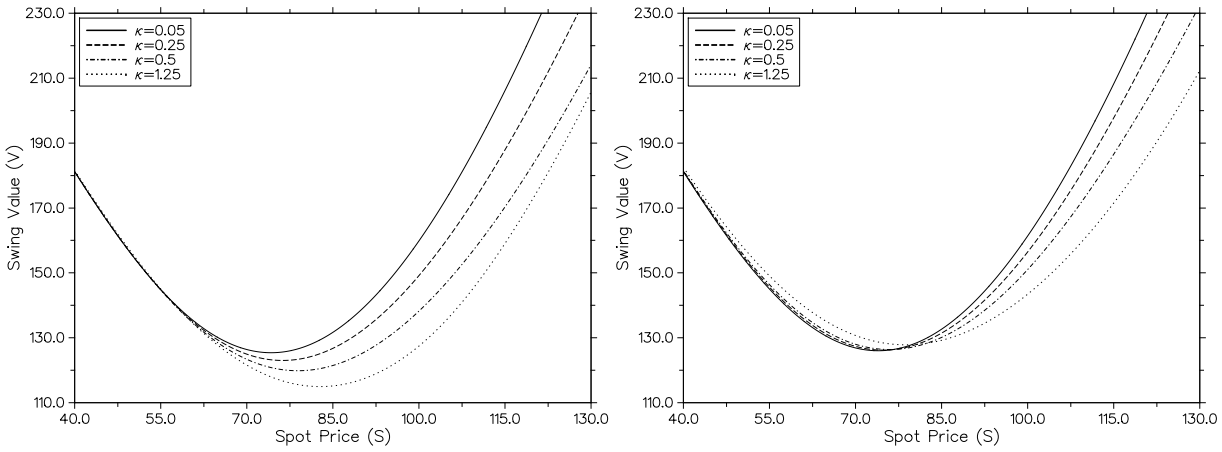

Figure 6. Effect of changing mean-reversion speed on value of a swing option. For the left plot, mean-reversion level $\theta = 80$, while for the right plot $\theta = 100$.

framework for valuing various vanilla and exotic options by transforming the pricing PIDE into the Fourier domain and performing a rescaling in frequency. We coin this method the mrFST method.

European, Bermudan and barrier contingent claims for four prototypical models were investigated to highlight the flexibility of both the model and the valuation framework. The method converges quickly, attaining second order convergence when pricing European, American and Bermudan options and first order convergence for barrier options. Moreover, European options are priced in one (or few in highly mean-reverting cases) iterations and no time-stepping is required between monitoring dates for Bermudan options. The mrFST method readily extends to multiple dimensions as we demonstrate by pricing European and barrier spread options. Moreover, we demonstrated how the method can be applied to swing options and this approach easily extends to storage, interruptible and other exotic option classes.

There are a number of interesting future directions for this research. Firstly, if the lifetime of the options are long, then regime changes may be necessary. In the original (without mean-reversion) FST method of Jackson, Jaimungal, and Surkov (2008), the authors extended the method to incorporate regime changes with a continuous time Markov chain as a driver of world states. We have already begun incorporating such generalizations of the multi-factor mean-reverting framework studied here. Further, it is possible to gain additional speed up in the convergence of American styled options by utilizing penalty methods. This requires modifying the underline PIDE so that exercise constraints are implicitly satisfied by a penalty term. Moreover, there is the very interesting and important work of calibrating the general model to market data. Some calibration has already been carried out by Paschke and Prokopczuk (2008) for Gaussian models, but generalizing to the

case with jumps will require the use of particle filters.

Finally, our models and valuation paradigm are very well suited for real option problems. The key concern here is the valuation of the option to invest in a project. Such project values typically mean-revert, as they are often linked to commodity prices. Much current and previous work focuses on analytical methods for infinite time horizon problems or using trees for finite time horizon problems when the underlying project value process is gaussian. Using our approach cointegration, jumps and finite lifetime can all be easily handled simultaneously. To this end, Jaimungal, de Souza, and Zubelli (2010) have applied the mrFST in the context of mean-reverting investment cost and project value. There are many other potential applications in the real option context.

A. Convergence Tables

A.1. Example 1 Convergence Results

N	Value	Change	Convergence	Time (msec.)
2048	16.62164063			2.613
4096	16.62117060	0.0004700		4.933
8192	16.62104004	0.0001306	1.8481	9.883
16384	16.62101181	0.0000282	2.2095	19.978
32768	16.62100608	0.0000057	2.2983	39.765

Table 1
Results for pricing *O1A-EUR* option under *M1A-MJD* model. Monte-Carlo price is 16.62372359 with 95% confidence interval width of 0.0289145 and requires 742 milliseconds.

N	Value	Change	Convergence	Time (msec.)
2048	9.62667912			2.609
4096	9.62572860	0.0009505		5.188
8192	9.62551724	0.0002114	2.1691	10.745
16384	9.62545443	0.0000628	1.7505	21.953
32768	9.62544341	0.0000110	2.5112	45.139

Table 2
Results for pricing *O1A-EUR* option under *M1B-KJD* model. Monte-Carlo price is 9.62716176 with 95% confidence interval width of 0.0157647 and requires 475 seconds.

N	M	Value	Change	Convergence	Time (sec.)
2048	256	18.31507922			0.050
4096	512	18.31471890	0.0003603		0.218
8192	1024	18.31462634	0.0000926	1.9609	0.905
16384	2048	18.31460293	0.0000234	1.9833	3.690
32768	4096	18.31459680	0.0000061	1.9324	15.630

Table 3
Results for pricing *O1B-AMR* option under *M1A-MJD* model. Monte Carlo price using $100,000$ sample paths and 10 replications is 18.1857 with 95% confidence interval width of 0.0224 and requires 1360 seconds.

N	M	Value	Change	Convergence	Time (sec.)
2048	256	15.52656184			0.047
4096	512	15.52704909	0.0004872		0.195
8192	1024	15.52716876	0.0001197	2.0255	0.911
16384	2048	15.52718115	0.0000124	3.2721	3.578
32768	4096	15.52718592	0.0000048	1.3754	14.983

Table 4
Results for pricing *O1B-AMR* option under *M1B-KJD* model. Monte Carlo price using $100,000$ sample paths and 10 replications is 15.4886 with 95% confidence interval width of 0.0129 and requires 1465 seconds.

N	M	Value	Change	Convergence	Time (sec.)
2048	252	2.75818698			0.048
4096	252	2.77495289	0.0167659		0.099
8192	252	2.77164607	0.0033068	2.3420	0.210
16384	252	2.77315499	0.0015089	1.1319	0.523
32768	252	2.77395701	0.0008020	0.9118	0.974

Table 5
Results for pricing *O1C-DBR* option under *M1A-MJD* model. Monte-Carlo price is 2.77533300 with 95% confidence interval width of 0.00323116 and requires 114 seconds.

N	M	Value	Change	Convergence	Time (sec.)
2048	252	2.95298034			0.047
4096	252	2.97243484	0.0194545		0.094
8192	252	2.96942825	0.0030066	2.6939	0.206
16384	252	2.97138302	0.0019548	0.6211	0.446
32768	252	2.97231665	0.0009336	1.0661	0.929

Table 6
Results for pricing *O1C-DBR* option under *M1B-KJD* model. Monte-Carlo price is 2.97503889 with 95% confidence interval width of 0.00266347 and requires 118 seconds.

A.2. Example 2 Convergence Results

N	Value	Change	Convergence	Time (sec.)
512^2	14.33440804			1.072
1024^2	14.30822752	0.0261805		5.018
2048^2	14.30115067	0.0070768	1.8873	21.587
4096^2	14.29924775	0.0019029	1.8949	90.429

Table 7
Results for pricing *O2-EUR* option under *M2-KJDD* model. Monte-Carlo price is 14.28324388 with 95% confidence interval width of 0.069424856 and requires 9.57 minutes.

N	Value	Change	Convergence	Time (sec.)
512^2	59.85324966			4.461
1024^2	59.69208506	0.1611646		21.028
2048^2	59.64885467	0.0432304	1.8984	88.082
4096^2	59.63823070	0.0106240	2.0247	352.491

Table 8
Results for pricing *O2-BRM* option under *M2-KJDD* model.

A.3. Example 3 Convergence Results

N	Value	Change	Convergence	Time (msec.)
512^2	29.90721436			0.835
1024^2	29.89801417	0.0092002		3.694
2048^2	29.89568844	0.0023257	1.9840	14.075
4096^2	29.89508556	0.0006029	1.9478	55.253

Table 9
Results for pricing *O3-ESPD* option under *M3-MJDGC* model. Monte-Carlo price is 29.88224191 with 95% confidence interval width of 0.05639975 and requires 20.8 minutes.

N	Value	Change	Convergence	Time (sec.)
512^2	33.24911959			1.457
1024^2	33.20574275	0.0433768		6.655
2048^2	33.19451206	0.0112307	1.9495	28.544
4096^2	33.19169324	0.0028188	1.9943	113.957

Table 10
Results for pricing *O3-BSPD* option under *M3-MJDGC* model.

A.4. Example 4 Convergence Results

N	Value	Change	Convergence	Time (sec.)
512^2	3.55378227			0.519
1024^2	3.55026668	0.0035156		2.215
2048^2	3.54939009	0.0008766	2.0038	8.941
4096^2	3.54917117	0.0002189	2.0015	36.542

Table 11
Results for pricing *O4-EUR* option under *M4-BMSM* model. Closed-form price is 3.54907367.

B. A Class of Risk-Neutral Measures

Since our market model is incomplete, there are many equivalent risk-neutral measures. In this section we provide a class of measure changes which preserves the real-world structure of model (2). To this end, consider the class of measure changes $\mathcal{Q}$ induced by the Radon-Nikodym derivative process

$$\begin{aligned}\left.\frac{d\mathbb{Q}}{d\mathbb{P}}\right|_{\mathcal{F}_t} = \exp\Bigg\{ & -\frac{1}{2}\int_0^t |\boldsymbol{\alpha}+\boldsymbol{\beta}\,\mathbf{Y}(s)|^2 ds + \int_0^t (\boldsymbol{\alpha}+\boldsymbol{\beta}\,\mathbf{Y}(s))\cdot d\mathbf{W}(s) \\ & - \int_0^t \int_{\mathbb{R}^d\setminus\{\mathbf{0}\}} \eta(\mathbf{Z})\,\nu(d\mathbf{Z}\times ds) + t\int_{\mathbb{R}^d\setminus\{\mathbf{0}\}} \ln(1+\eta(\mathbf{Z}))\,\mu(d\mathbf{Z})\Bigg\}\,.\end{aligned} \tag{36}$$

Here, $\boldsymbol{\alpha}$ is a d-dimensional constant vector, $\boldsymbol{\beta}$ is $d\times d$ constant matrix and $\eta(\mathbf{Z})$ is an arbitrary function satisfying the integrability conditional that $\exists\ \mathbf{c},\ c_i>0$ s.t. $\int_{\mathbb{R}^d\setminus\{\mathbf{0}\}}(e^{\mathbf{c}\cdot\mathbf{Z}}-1)\ln(1+\eta(\mathbf{Z}))\,\nu(d\mathbf{Z})<+\infty$. The parameters $\boldsymbol{\alpha}$ and $\boldsymbol{\beta}$ together with the function $\eta(\mathbf{Z})$ provide significant flexibility in the class of equivalent risk-neutral measures.

Clearly, (36) factors into independent diffusive and jump components and a straightforward application of Girsanov's theorem implies that the processes

$$\widehat{\overline{\mathbf{W}}}(t) = -\int_0^t (\boldsymbol{\alpha}+\boldsymbol{\beta}\mathbf{Y}(s))\,ds + \overline{\mathbf{W}}(t) \tag{37}$$

are independent Brownian motions under the new measure $\mathbb{Q}$, where $\overline{\mathbf{W}}_t = \mathbf{U}^{-1}\mathbf{W}(t)$ and $\mathbf{U}$ is the Cholesky decomposition of the covariance matrix $\boldsymbol{\Sigma}$ so that $\boldsymbol{\Sigma}=\mathbf{U}\mathbf{U}'$. Furthermore,

$$\widehat{\mathbf{L}}(t) = \int_0^t \int_{\mathbb{R}^d\setminus\{\mathbf{0}\}} \mathbf{Z}\,\mu(d\mathbf{Z}\times ds) \tag{38}$$

is a d-dimensional pure jump process with $\mathbb{Q}$-compensator

$$\widehat{\nu}(d\mathbf{Z}\times ds) = (1+\eta(\mathbf{Z}))\,\nu(d\mathbf{Z}\times ds)\,. \tag{39}$$

Consequently, the dynamics of $\mathbf{Y}(t)$ can then be written as

$$\begin{aligned} d\mathbf{Y}(t) &= -\boldsymbol{\kappa}\mathbf{Y}(t_-)dt + d\mathbf{J}(t) \\ &= (\boldsymbol{\gamma}-\boldsymbol{\kappa}\mathbf{Y}(t_-))dt + \mathbf{U}d\overline{\mathbf{W}}(t) + d\mathbf{L}(t) \\ &= \widehat{\boldsymbol{\kappa}}(\widehat{\boldsymbol{\kappa}}^{-1}(\boldsymbol{\gamma}-\widehat{\boldsymbol{\gamma}}+\mathbf{U}\boldsymbol{\alpha})-\mathbf{Y}(t))dt + \widehat{\gamma}\,dt + \mathbf{U}\widehat{\overline{\mathbf{W}}}(t) + d\widehat{\mathbf{L}}(t)\,, \end{aligned} \tag{40}$$

where $\widehat{\boldsymbol{\kappa}} = \boldsymbol{\kappa}-\mathbf{U}\boldsymbol{\beta}$ and $\widehat{\gamma}_i = -\int_{\mathbb{R}\setminus\{0\}} z_i\,\nu(dz_i)$. Now define the shifted process $\widehat{\mathbf{Y}}(t) = \mathbf{Y}(t) -$

$\widehat{\boldsymbol{\kappa}}^{-1}(\boldsymbol{\gamma} - \widehat{\boldsymbol{\gamma}} + \mathbf{U}\boldsymbol{\alpha})$, then we have

$$d\widehat{\mathbf{Y}}(t) = -\widehat{\boldsymbol{\kappa}}\widehat{\mathbf{Y}}(t)\,dt + d\widehat{\mathbf{J}}(t)\,, \tag{41a}$$

$$\mathbf{X}(t) = \widehat{\boldsymbol{\theta}}(t) + \mathbf{B}\widehat{\mathbf{Y}}(t)\,. \tag{41b}$$

Here, $\widehat{\boldsymbol{\theta}}(t) = \boldsymbol{\theta}(t) + \widehat{\boldsymbol{\kappa}}^{-1}(\boldsymbol{\gamma} - \widehat{\boldsymbol{\gamma}} + \mathbf{U}\boldsymbol{\alpha})$ and $\widehat{J}(t) = \mathbf{U}\widehat{\overline{\mathbf{W}}}(t) + \widehat{L}(t)$ – a Lévy process with $\mathbb{Q}$ Lévy triple $(\widehat{\boldsymbol{\gamma}}, \boldsymbol{\Sigma}, \widehat{\boldsymbol{\nu}})$. To keep the model for $\widehat{\mathbf{Y}}$ mean-reverting, it is necessary to constrain the coefficient β such that $\widehat{\boldsymbol{\kappa}}$ has positive eigenvalues.

Notice that under this class of measure changes, the risk-neutral dynamics (41) is of the exact same form as the real world dynamics (2), however, the mean-reverting rate, mean-revering level and jump measure are altered. From the above representation it is clear that $\eta(\mathbf{Z})$ is responsible for altering the distribution of jumps, $\boldsymbol{\beta}$ is responsible for altering the rate of mean-reversion and $\boldsymbol{\alpha}$ is responsible for altering the level of mean-reversion (all else being zero). Since the structure is preserved, we choose to use the same labels for the $\mathbb{P}$ and $\mathbb{Q}$ parameters in the main text as the context dictates which measure is relevant. In particular, from Theorem 2.1 onwards all parameters are risk-neutral ones.

C. Proof of Theorem 2.1

The fundamental theorem of asset pricing implies that the discounted price process $v(t, \mathbf{Y}(t)) \triangleq e^{r(T-t)}\,V(t, \mathbf{Y}(t))$ is a martingale under a, not necessarily unique, risk-neutral measure $\mathbb{Q}$. As discussed in the previous Appendix, we have chosen a particular class of measures $\mathcal{Q}$ which preserves the structure of our real-world model and will pick one of these measures $\mathbb{Q} \in \mathcal{Q}$ to work with. Consequently, the price must satisfy the PIDE

$$\begin{cases} (\partial_t + \mathcal{L})v(t, \mathbf{y}) = 0\,, \\ \qquad v(T, \mathbf{y}) = \phi(\mathbf{S}(0)e^{\boldsymbol{\theta} + \mathbf{B}\mathbf{y}})\,, \end{cases} \tag{42}$$

where the $\mathcal{L}$ is the infinitesimal generator of the $\mathbf{Y}_t$ process and acts on twice differentiable functions $f(y)$ as follows:

$$\mathcal{L} = (\boldsymbol{\gamma} - \boldsymbol{\kappa}\mathbf{y})'\partial_{\mathbf{y}} + \tfrac{1}{2}\partial_{\mathbf{y}}'\boldsymbol{\Sigma}\partial_{\mathbf{y}} + \int_{\mathbb{R}^d/\{0\}} \left[f(\mathbf{y} + \mathbf{z}) - f(\mathbf{y}) - \mathbf{1}_{\{|\mathbf{z}|<1\}}\mathbf{z}'\partial_{\mathbf{y}} f\right] \nu(d\mathbf{z})\,. \tag{43}$$

Transforming (42) into the Fourier domain $v(t, \mathbf{y}) \mapsto \mathcal{F}[v(t,\cdot)](\boldsymbol{\omega})$ leads to

$$\begin{cases} (\partial_t + \boldsymbol{\omega}'\boldsymbol{\kappa}\partial_{\boldsymbol{\omega}} + \psi(\boldsymbol{\omega}) + \operatorname{Tr}\boldsymbol{\kappa})\mathcal{F}[v(t,\cdot)](\boldsymbol{\omega}) = 0\,, \\ \qquad\qquad \mathcal{F}[v(T,\cdot)](\boldsymbol{\omega}) = \mathcal{F}[\phi](\boldsymbol{\omega})\,. \end{cases} \tag{44}$$

Here, $\psi(\boldsymbol{\omega})$ is the characteristic exponent defined in (16). Introducing the new coordinate system

$$\mathcal{F}[\tilde{v}(t,\cdot)](\boldsymbol{\omega}) = \mathcal{F}[v(t,\cdot)](e^{-\boldsymbol{\kappa}'(T-t)}\,\boldsymbol{\omega}) \;, \tag{45}$$

reduces the PDE (44) to an ODE in time for every $\boldsymbol{\omega}$:

$$\begin{cases} (\partial_t + \psi(e^{-\boldsymbol{\kappa}'(T-t)}\boldsymbol{\omega}) + \operatorname{Tr}\boldsymbol{\kappa})\mathcal{F}[\tilde{v}(t,\cdot)](\boldsymbol{\omega}) = 0 \;, \\ \qquad\qquad\qquad\qquad \mathcal{F}[\tilde{v}(T,\cdot)](\boldsymbol{\omega}) = \mathcal{F}[\tilde{\phi}](\boldsymbol{\omega}) \;. \end{cases} \tag{46}$$

This ODE is easily solved and after changing coordinates back to the original ones and taking inverse Fourier transforms we arrive at the required result. □

References

Andersen, L. and J. Andreasen (2000). Jump-diffusion processes: Volatility smile fitting and numerical methods for option pricing. *Review of Derivatives Research 4*, 231–262.

Barlow, M., Y. Gusev, and M. Lai (2004). Calibration of multifactor models in electricity markets. *International Journal of Theoretical and Applied Finance 7*(2), 101–120.

Benth, F. E., J. S. Benth, and S. Koekebakker (2008). *Stochastic Modeling of Electricity and Related Markets*. Advanced Series on Statistical Science and Applied Probability. World Scientific.

Benth, F. E., J. Kallsen, and T. Meyer-Brandis (2007). A non-gaussian Ornstein-Uhlenbeck process for electricity spot price modeling and derivatives pricing. *Applied Mathematical Finance 14*(2), 153–169.

Benth, F. E. and R. Kufakunesu (2009). Pricing of exotic energy derivatives based on arithmetic spot models. *International Journal of Theoretical and Applied Finance (IJTAF) 12(4)*, 491–506.

Briani, M., R. Natalini, and G. Russo (2004). Implicit-explicit numerical schemes for jump-diffusion processes. IAC Report 38, Istituto per le Applicazioni del Calcolo IAC-CNR.

Carr, P. and D. B. Madan (1999). Option valuation using the fast Fourier transform. *The Journal of Computational Finance 2*(4), 61–73.

Carriere, J. (1996). Valuation of the early-exercise price for options using simulations and non-parametric regression. *Insurance: Mathematics and Economics 19*(1), 19–30.

Cartea, A. and M. Figueroa (2005). Pricing in electricity markets: a mean reverting jump diffusion model with seasonality. *Applied Mathematical Finance 22*(4), 313–335.

Cartea, A. and C. González-Pedraz (2010). How much should we pay for interconnecting electricity markets? a real options approach. *Available at SSRN: http://ssrn.com/abstract=1639360*.

Chen, Z. and P. Forsyth (2007). Implications of a regime-switching model on natural gas storage valuation and optimal operation. Preprint.

Clewlow, L. and C. Strickland (2000). *Energy Derivatives: Pricing and Risk Management*. Lacima Publications.

Cortazar, G. and E. Schwartz (1994). The valuation of commodity contingent claims. *The Journal of Derivatives 1*, 27–29.

d'Halluin, Y., P. A. Forsyth, and K. R. Vetzal (2005). Robust numerical methods for contingent claims under jump diffusion processes. *IMA Journal of Numerical Analysis 25*, 87–112.

Duffie, D., J. Pan, and K. Singleton (2000). Transform analysis and asset pricing for affine jump-diffusions. *Econometrica 68*, 1343–1376.

Eydeland, A. and K. Wolyniec (2003). *Energy and Power Risk Management*. John Whiley and Sons.

Gibson, R. and E. Schwartz (1990). Stochastic convenience yield and the pricing of oil contingent claims. *The Journal of Finance 45*, 959–976.

Hikspoors, S. and S. Jaimungal (2007). Energy spot price models and spread options pricing. *International Journal of Theoretical & Applied Finance 10(7)*, 1111–1135.

Jackson, K. R., S. Jaimungal, and V. Surkov (2008). Fourier space time-stepping for option pricing with Lévy models. *The Journal of Computational Finance 12*(2), 1–28.

Jaimungal, S., M. O. de Souza, and J. Zubelli (2010). Real option valuation with uncertain costs.

Kou, S. G. (2002). A jump-diffusion model for option pricing. *Management Science 48*(8), 1086–1101.

Longstaff, F. and E. Schwartz (2001). Valuing american options by simulation: a simple least-squares approach. *Review of Financial Studies 14*(1), 113–147.

Lord, R., F. Fang, F. Bervoets, and K. Oosterlee (2008). A fast and accurate FFT-based method for pricing early-exercise options under Lévy processes. *SIAM Journal on Scientific Computing 30*(4), 1678–1705.

Merton, R. C. (1976). Option pricing when underlying stock returns are discontinuous. *Journal of Financial Economics 3*, 125–144.

Paschke, R. and M. Prokopczuk (2008). Integrating multiple commodities in a model of stochastic price dynamics.

Press, W. H., S. A. Teukolsky, W. T. Vetterling, and B. P. Flannery (1992). *Numerical Recipes in C: The art of scientific computing*. Cambridge University Press.

Sato, K.-I. (1999). *Lévy Processes and Infinitely Divisible Distributions*. Cambridge Studies in Advanced Mathematics. Cambride University Press.

Schwartz, E. (1997). The stochastic behavior of commodity prices: implications for valuation and hedging. *The Journal of Finance 52*(3), 923–973.

Schwartz, E. S. and J. E. Smith (2000). Short-term variations and long-term dynamics in commodity prices. *Management Science 46(7)*, 893–911.

Ware (2005). Swing options in a mean-reverting world. Presentation at: Stochastic Calculus and its applications to Quantitative Finance and Electrical Engineering, a conference in honour of Robert Elliott, Calgary.